14th World Congress on Computational Mechanics (WCCM)
ECCOMAS Congress 2020)
Virtual Congress: 11-–15 January 2021
F. Chinesta, R. Abgrall, O. Allix and M. Kaliske (Eds)

CRACK-TRACKING IN THE REGULARIZED XFEM: A VIABLE ALTERNATIVE TO NONLOCAL AND COHESIVE ZONE MODELS

ELENA BENVENUTI*[1], NICOLA ORLANDO [1]

[1] Department of Engineering, University of Ferrara
via Saragat, 1, 44122, Ferrara, Italy
elena.benvenuti@unife.it, nicola.orlando@unife.it

Key words: Crack tracking, quasi-brittle materials, damage, continuous-discontinuous transition

Abstract. We have devised a crack-tracking methodology for general crack paths in elasto-damaging materials based on the regularized extended finite element method. The resulting procedure is in-between nonlocal models, where the discontinuity surface is replaced by a finite width zone, and cohesive zone models, where the discontinuous regime is governed by a traction-separation law.

1 INTRODUCTION

We propose an original methodology to track general crack paths in elastodamaging bulks in the framework of the regularized extended finite element technology [1]. The approach can be regarded as an example of continuous-discontinuous transitioning procedure. Existing transitioning procedures provide a bridge between continuum models, such as smeared crack [2], nonlocal [3], and phase-field models [4, 5], and discrete formulations, such as interface and cohesive zone models [6], extended and generalized finite elements [7]. Our approach is different and can be likened to nonlocal and phase field approaches at the onset of the cracking process, while it converges to the same results as cohesive zone models for vanishing regularization length.

The extended finite element method enriches the space of standard partition-of-unity shape functions with functions displaying the mathematical structure of the searched solution [7]. It allows to capture cracks and discontinuities without mesh adaptivity. The extended finite element method has significantly progressed in the field of crack propagation [8], often in combination with crack tracking algorithms [9], and has been successfully integrated within continuous-discontinuous transition procedures [10].

The regularized extended finite element method [1] was previously restricted to *a priori* known discontinuities [11, 12, 13, 14, 15]. Here, we aim to capture general crack paths [16]. The idea is to let the local damage model build the strain localization band. Then, as soon as a critical condition is achieved, the regularized extended finite element method is adopted in the pre-determined strain localization band. On the one hand, the width of the localization band is strictly controlled by the regularization procedure, i.e. it cannot either prematurely vanish or spuriously increase. On the other hand, the model captures a strong discontinuity kinematics as soon as the structural strength is completely exhausted.

In the current regularized extended finite element model, the transition to the discontinuous formulation is activated at the early stages of the damaging process, while local constitutive laws are used up to

the transition. Two internal lengths are introduced: a minimum length related to the final width of the crack in the late stages of the process and one maximum length that imposes the minimum distance between two adjacent cracks. The former width should be taken as small as possible consistently with the resolution of the finite element mesh, while the latter one is related to the width of the process zone of the material intended as the zone where the fracture energy should be dissipated during the whole cracking process.

Furthermore, the present regularized extended finite element formulation is endowed with a crack density function evolving with the damage of the underlying bulk, like phase-field models, and limits the width of the strain localization band, analogously to nonlocal models. Remarkably, the present formulation lacks of the damage broadening effect typical of nonlocal models. The resulting framework can be regarded as a unique and original contribution in virtue of the development of a flexible direction tracking procedure and the dynamic handling of the width of the process zone based on the damage level.

This contribution contains a basic presentation of the discrete form of the adopted kinematics, damage evolution and variational formulation. Then, the crack tracking procedure is discussed and, finally, applied to the simulation of a two-dimensional pre-notched plate.

1.1 The regularized formulation of the problem of a cracked body

In the forthcoming developments, we adopt a bold vector notation and restrict to the case where the crack is a line. Let the displacement field $\boldsymbol{u}$ be defined over the domain $\Omega \subset \mathbb{R}_3$ with boundary $\partial\Omega$, and $\bar{\boldsymbol{u}}$ be the displacement on $\partial\Omega_d \subset \partial\Omega$. We assume $\boldsymbol{u}$ to exhibit a jump $[\![\boldsymbol{u}]\!] = \boldsymbol{u}^+ - \boldsymbol{u}^-$ across the crack Γ, $\boldsymbol{u}^+$ and $\boldsymbol{u}^-$ being the traces of $\boldsymbol{u}$ on the opposite sides of Γ. We postulate the existence of a stress field $\boldsymbol{\sigma}$ and allow the exchange of cohesive forces $\boldsymbol{\sigma n} = \boldsymbol{f}_s$ across a certain portion Γ_s in front of the crack line Γ, while tractions are not transmitted across the fully developed discontinuity line Γ_c, being $\Gamma = \Gamma_c \cup \Gamma_s$. Let $\boldsymbol{n}$ be a field representative of the normal versor to the boundary and the crack Γ. We aim to solve the problem of the equilibrium of the cracked body Ω subjected to appropriate boundary conditions and write the equations representative of the problem at hand as:

$$\begin{aligned} &\mathrm{div}\boldsymbol{\sigma} = 0 \text{ in } \Omega \setminus \Gamma, \quad && \boldsymbol{\sigma n} = \bar{\boldsymbol{p}} \text{ in } \partial\Omega_p \setminus \Gamma, \\ &\boldsymbol{\sigma n} = f_s \text{ on } \Gamma_s, && \boldsymbol{\sigma n} = 0 \text{ on } \Gamma_c \\ &\boldsymbol{u} = \bar{\boldsymbol{u}} \text{ on } \partial\Omega_u \setminus \Gamma. \end{aligned} \tag{1}$$

We search for a discontinuous solution of problem (1) among the set of vector displacement cast as

$$\boldsymbol{u} = \boldsymbol{v} + H[\![\boldsymbol{u}]\!], \tag{2}$$

where H is the Heaviside function that is defined as $H(s(\boldsymbol{x})) = 1$ if $x \in \Gamma$ and $H = 0$ if $x \neq \Gamma$. The signed distance function of $\boldsymbol{x}$ with respect to the crack line Γ is computed as $s(\boldsymbol{x}) = \|\boldsymbol{x} - \bar{\boldsymbol{x}}\| S(\boldsymbol{x} - \bar{\boldsymbol{x}})$, where $\bar{\boldsymbol{x}}$ is the closest point projection of $\boldsymbol{x}$ onto Γ and S is a Boolean that takes values ± 1.

We reckon that the space the displacement field belongs to should be appropriately chosen and that the proper variational formulation descends from the theory of free-discontinuity problems formulated for fields with jumps [17]. In particular, we recognize that $\boldsymbol{u}$ in Eq. (2) descends from the fields belonging to space of special functions of bounded variation SBV [18], and the first variation is

$$D\boldsymbol{u} = \nabla \boldsymbol{v} + H\nabla[\![\boldsymbol{u}]\!] + \delta_\Gamma\big([\![\boldsymbol{u}]\!] \otimes_s \boldsymbol{n}\big), \tag{3}$$

where the derivative of H is a distributional function, the Dirac delta function δ_Γ. In this context, worth noting results have been achieved exploiting regularized functionals $\Gamma-$converging to the Mumford-Shah functional such as the Ambrosio-Tortorelli functional [17]

$$G_\eta(u,v) = \int_\Omega v^2 |\nabla u|^2 dx + \frac{1}{2}\int_\Omega \left[\eta|\nabla v|^2 + \frac{1}{\eta}(1-v)^2\right] dx, \tag{4}$$

defined on functions u, v such that $(u,v) \in (H^1(\Omega,\mathbb{R}^m) \times H^1(\Omega))$, and $\eta \leq v \leq 1$. Here, the variable v is chosen to tend to take the value 1 almost everywhere and the value 0 on Γ. Noteworthy, the second integral converges to a surface energy concentrating on the jump set Γ. It is this property that allows the development of consistent variational formulations for fractured bodies based on functional (4).

In the wake of [17], we reformulate problem (1) and introduce a regularized version of the kinematics. In particular, we approximate $\boldsymbol{u}$ through a regularized differentiable function $\boldsymbol{u}_\rho$ converging to $\boldsymbol{u}$ for vanishing ρ. For this purpose, we replace the Heaviside function H with a regularized version H_ρ. Thus the regularised displacement field $\boldsymbol{u}_\rho$ takes the form

$$\boldsymbol{u}_\rho(\boldsymbol{u},v) = \boldsymbol{v} + H_\rho \boldsymbol{j}, \qquad \lim_{\rho\to 0} \boldsymbol{u}_\rho = \boldsymbol{u}. \tag{5}$$

For instance, we have cast

$$H_\rho(s(\boldsymbol{x})) = \frac{1}{V_\rho}\int_0^{s(\boldsymbol{x})} \mathcal{W}_\rho(\xi) d\xi, \tag{6}$$

where $\mathcal{W}_\rho$ represents a weight function centered at Γ and $V_\rho = \int_\Omega \mathcal{W}_\rho(\xi) d\xi$. In particular, we have adopted the weight function $\mathcal{W}_\rho(\xi) = e^{-\frac{|\xi|}{\rho}}$ [1]. The displacement profile tends to a jump behind the crack line and to a regularised profile in the front of Γ.

Width of the regularized damage band The regularized Heaviside H_ρ has a support whose width is expected to shrink as the damaging process advances. This effect is reached by modulating the regularization length according to the damage level as follows [11].

We define two regularization lengths, namely ρ_m and ρ_M, which represent the minumum and the maximum value that ρ can take. The value of ρ is assumed being a function decreasing with the value of the damage d_ρ according to the following law:

$$\rho = \begin{cases} \rho_M & \text{for } d_\rho = d_m, \\ \alpha d_\rho + \beta & d_m \leq d_\rho \leq d_M, \\ \rho_m & \text{for } d_\rho \geq d_M, \end{cases} \tag{7}$$

where $\alpha = \dfrac{\rho_m - \rho_M}{d_M - d_m}$ and $\beta = \dfrac{d_M\rho_M - d_m\rho_m}{d_M - d_m}$. The law (7) describes a three-stages evolution of ρ, starting from a maximal value ρ_M, linearly decreasing between d_m and d_M, with $d_m \leq d_M$, up to assuming the minimum value ρ_m for $d > d_M$.

By compatibility, the variation of $\boldsymbol{u}_\rho$ reads

$$D\boldsymbol{u}_\rho = \nabla \boldsymbol{v} + H_\rho \nabla \boldsymbol{j} + \delta_\rho(\boldsymbol{n} \otimes_s \boldsymbol{j}), \tag{8}$$

where the term $\delta_\rho = \|\nabla H_\rho\|$ denotes the norm of the derivative of H_ρ. δ_ρ is localized within a crack band whose width corresponds to the support of the regularization. The support of δ_ρ noncompact, and it is necessary to introduce a truncation length beyond which the value of δ_ρ is not to be evaluated. We found [19] that a truncated support length of 40ρ provides a satisfying compromise between computational burden and accuracy, at least for the present H_ρ. In the following developments, the lengths $\ell_{\rho,M}$ and $\ell_{\rho,m}$ will denote the width of the truncated supports of δ_ρ for $\rho = \rho_M$ and $\rho = \rho_m$, respectively. Since we consider linear elasticity, in the previous equation, we restrict the approximate gradients to their symmetric part. For this reason, $\boldsymbol{n} \otimes_s \boldsymbol{a}$ denotes the symmetric part of tensor $\boldsymbol{n} \otimes \boldsymbol{a}$. Function δ_ρ can be recognized as the crack field density and plays a role analogous to the crack density of phase-field models.

1.2 Space discretization

Following the extended finite element method [7], the discrete displacement in the enriched elements is approximated by means of the shifted basis approach [20] as:

$$\boldsymbol{u}_h(\boldsymbol{x}) = \sum_{I \in \mathcal{N}} N_I(\boldsymbol{x}) \boldsymbol{v}_I + \sum_{I \in \mathcal{N}_{enr}} N_I(\boldsymbol{x}) \big(H_\rho(s(\boldsymbol{x})) - H_{\rho,I}\big) \boldsymbol{j}_I, \tag{9}$$

where $\mathcal{N}_{enr}$ denotes the number of enriched nodes, $H_{\rho,I} = H_\rho(s(\boldsymbol{x}_I))$, and $\boldsymbol{v}_I$ and $\boldsymbol{j}_I$ are the *nodal* vector variables of the standard part of the displacement and the enrichment, respectively. For the sake of simplicity, we have here chosen the same shape functions N for both the standard degrees of freedom in $\mathcal{N}$ and the enriched degrees of freedom associated with $\mathcal{N}_{enr}$. The discretization (9) leads to define the set of elements crossed by the crack line, and the set of enriched elements whose distance from the crack line is smaller or equal to the semi-support width ℓ_ρ but are not crossed by the crack line. The remaining elements are not enriched and are governed by a standard finite element approximation.

Let $\boldsymbol{V}$ and $\boldsymbol{J}$ be the vectors collecting the nodal degrees of freedom, and $\boldsymbol{B}$ and $\bar{\boldsymbol{N}}$ denote the compatibility matrices. Then the discrete form of the strain and stress fields can be written in the compact form

$$\begin{aligned} \boldsymbol{\varepsilon}_h(\boldsymbol{x}) &= \boldsymbol{B}(\boldsymbol{x})\boldsymbol{V} + \hat{H}_\rho(s(\boldsymbol{x}))\boldsymbol{J}, & \boldsymbol{\varepsilon}_{\rho,h}(\boldsymbol{x}) &= \delta_\rho(\boldsymbol{x})\bar{\boldsymbol{N}}(\boldsymbol{x})\boldsymbol{J}, \\ \boldsymbol{\sigma}_h(\boldsymbol{x}) &= \boldsymbol{B}(\boldsymbol{x})\boldsymbol{C}_d\big(\boldsymbol{V} + \hat{H}_\rho(s(\boldsymbol{x}))\boldsymbol{J}\big), & \boldsymbol{\sigma}_{\rho,h}(\boldsymbol{x}) &= \boldsymbol{C}_\rho\bar{\boldsymbol{N}}(\boldsymbol{x})\boldsymbol{J}, \end{aligned} \tag{10}$$

where we have set $\boldsymbol{C}_d = (1-d)\boldsymbol{C}$ and $\boldsymbol{C}_\rho = (1-d_\rho)\bar{\boldsymbol{C}}$ and d and d_ρ are damage variables that wil be defined in the following section. Finally, $\hat{H}_\rho$ denotes the shifted regularized Heaviside function.

1.3 Time discrete formulation and damage evolution

Let the loading history from instant t^0 to the time instant t^N be subdivided into N non-overlapping intervals, $[t^0, t^N] = \bigcup_{n=1,N}[t^{n-1}, t^n]$. Given $\boldsymbol{\varepsilon}^{n-1}$ and $\boldsymbol{\varepsilon}_\rho^{n-1}$ at instant t^{n-1}, so that d^{n-1} and d_ρ^{n-1} are known, at the end of next load step during the interval $[t^{n-1}, t^n]$, we compute $\boldsymbol{v}^n$ and $\boldsymbol{j}^n$ and update the values of the damage, d^n and d_ρ^n, following the classic Backward Euler integration scheme.

First, we define an appropriate effective stress for the evolution of d and associate another one with the evolution d_ρ as

$$\tilde{\boldsymbol{\sigma}}^n = \boldsymbol{C}^n \nabla \boldsymbol{v}^n, \qquad \tilde{\boldsymbol{\sigma}}_\rho^n = w_\rho(s(\boldsymbol{x}))\boldsymbol{C}^n(\boldsymbol{n} \otimes_s \boldsymbol{j}^n), \tag{11}$$

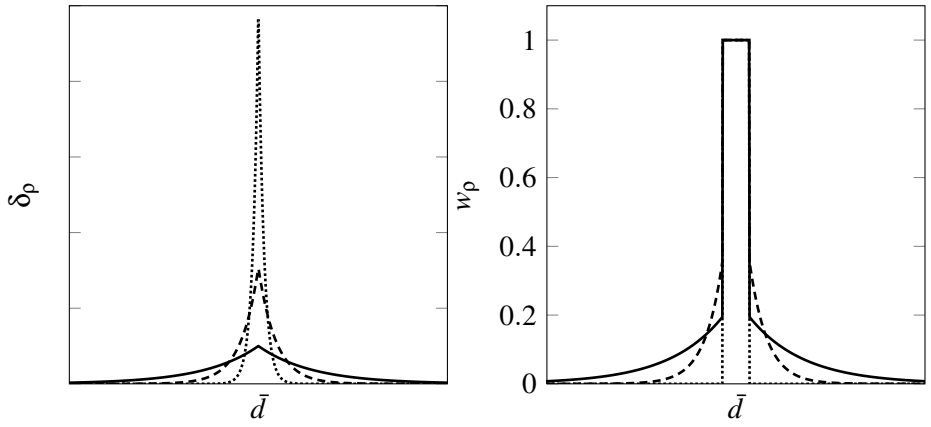

(a) (b)

Figure 1: Crack density function δ_ρ (a) and weight function w_ρ (b) for variable ρ; the continuous line indicates ρ_M, the dashed line refers to $\rho_m < \rho < \rho_M$, and the dotted line to $\rho = \rho_m$.

respectively. Here, function w_ρ plays the role of a weight function of the signed distance $s(\boldsymbol{x})$ and is cast as

$$w_\rho(s(\boldsymbol{x})) = \begin{cases} 1 & s(\boldsymbol{x}) \leq \ell_{\rho_m}/2, \\ \delta_\rho & s(\boldsymbol{x}) > \ell_{\rho_m}/2. \end{cases} \tag{12}$$

The adoption of w_ρ makes it possible to carry out the transition from a thick to a thin process zone, and overcomes a limitation inherent in the previous version of the regularized extended finite element [11]. A plot of w_ρ for variable values of ρ is shown in Fig. 1b.

We assume an isotropic damage Rankine model, where at each Gauß point the loading functions at the current instant t^n read

$$g^n = \tau(\boldsymbol{\varepsilon}^n) - \kappa^n, \qquad g^n_\rho = \tau_\rho(\boldsymbol{\varepsilon}^n_\rho) - \kappa^n_\rho. \tag{13}$$

Here, thresholds κ^n and κ^n_ρ are the maximum values that equivalent stress scalars have ever reached during the loading history up to the current instant t_{n+1} as follows

$$\kappa^n(\boldsymbol{\varepsilon}^n) = \sup_{i\in[0,n]} \{\tau(\boldsymbol{\varepsilon}^i)\}, \qquad \kappa^n_\rho(\boldsymbol{\varepsilon}^n_\rho) = \sup_{i\in[0,n]} \{\tau_\rho(\boldsymbol{\varepsilon}^i_\rho)\}. \tag{14}$$

Moreover, τ^n and τ^n_ρ are equivalent stress scalars defined as:

$$\tau^n = \langle \max(\mathrm{eig}(\tilde{\boldsymbol{\sigma}}^n)) \rangle, \qquad \tau^n_\rho = \langle \max(\mathrm{eig}(\tilde{\boldsymbol{\sigma}}^n_\rho)) \rangle, \tag{15}$$

where the Macaulay brackets $\langle\cdot\rangle$ are such that $\langle x \rangle$ is the ramp function.

Since κ and κ_ρ are non-decreasing functions of the strain fields, the rate form of the loading unloading conditions can be integrated over the time. Therefore, the damage variables increase monotonically with the equivalent stress, and thus, with the current damage threshold κ and κ_ρ [21]. In particular, the damage variables evolve as non-decreasing functions of the associated damage thresholds through the

relationships

$$d^n = \begin{cases} d^{n-1} & \text{if } \kappa^n < \kappa^{n-1}, \\ G(\kappa^n) & \text{if } \kappa^n \geq \kappa^{n-1} \text{ and } G(\kappa^n) \leq d_m, \\ d_m & \text{if } G(\kappa^n) > d_m, \end{cases} \qquad d_\rho^n = \begin{cases} d_m & \text{if } G(\kappa_\rho^n) < d_m, \\ d_\rho^{n-1} & \text{if } \kappa_\rho^n < \kappa_\rho^{n-1}, \\ G(\kappa_\rho^n) & \text{if } \kappa^n \geq \kappa_\rho^{n-1}. \end{cases} \tag{16}$$

where a necessary condition to transition from the continuous to the discontinuous setting is that $d = d_m$. Specifically, we have adopted for G the following exponential law [22]

$$G(\tilde{\kappa}) = 1 - \frac{\tilde{\kappa}_0}{\tilde{\kappa}} e^{h(\tilde{\kappa})}, \; h(\tilde{\kappa}) = -2H \frac{\tilde{\kappa} - \tilde{\kappa}_0}{\tilde{\kappa}_0}, \tag{17}$$

where H is a hardening modulus, $\tilde{\kappa}$ is the current threshold and $\tilde{\kappa}_0$ is an initial threshold that is a material parameter.

The space-time discrete form of the work principle is cast as [1]:

$$\int_\Omega \boldsymbol{C}_d^n \boldsymbol{B}(\boldsymbol{V}^n + H_\rho \boldsymbol{J}^n) \cdot \boldsymbol{B}(\tilde{\boldsymbol{V}}^n + H_\rho \tilde{\boldsymbol{J}}^n) dV + \int_\Omega \delta_\rho \bar{\boldsymbol{N}} \boldsymbol{J}^{T,n} \cdot \boldsymbol{C}_\rho^n \bar{\boldsymbol{N}} \tilde{\boldsymbol{J}}^n dV = \int_{\partial\Omega_p \setminus \Gamma} \boldsymbol{F}^n \cdot \boldsymbol{N} \tilde{\boldsymbol{V}}^n dS, \tag{18}$$

where $\tilde{\boldsymbol{V}}$ and $\tilde{\boldsymbol{J}}$ are arbitrary variations and the damage variables are computed by means of the loading-unloading conditions (16). In virtue of the arbitrariness of $\tilde{\boldsymbol{V}}$ and $\tilde{\boldsymbol{J}}$, the solving system of equations is obtained. We have proved that the second term at the l.h.s of the previous equation converges to the traction-separation law for vanishing ρ [1], namely

$$\lim_{\rho \to 0} \int_\Omega \delta_\rho \bar{\boldsymbol{N}} \boldsymbol{J}^{T,n} \cdot \boldsymbol{C}_\rho^n \bar{\boldsymbol{N}} \tilde{\boldsymbol{J}}^n dV = \int_\Gamma \boldsymbol{\sigma}^n \boldsymbol{n} \cdot [\![\boldsymbol{u}]\!]^n dS. \tag{19}$$

This property allows us to establish a close relationship between the adopted approach and cohesive zone models. The solution is computed through a Newton-Raphson iterative procedure, the loading increments being applied via an arc-length algorithm with indirect control of purposely selected monotonically increasing degrees of freedom.

2 Crack tracking algorithm

The level set method is the traditional tool that allows the extended finite element to track the surfaces of discontinuities and singularities. In the present case, the crack surface evolves piecewisely by incrementally adding crack segments to the crack path crystallized at the previous time step. Hence, the crack level set and the geometry of the consolidated crack path have to be stored in the crossed elements. The vector level set method [20] allows to easily store the geometric data describing the evolution of the crack line in two-dimensions as a vector consisting of the sign of the signed distance from the crack line and the coordinates of the closest point projection vector.

2.1 Crack evolution

Let Γ^{n-1} and Ω_ρ^{n-1} be the crack line and the associated regularised crack domain at instant t^{n-1}, respectively. After a time interval $\Delta t = [t^{n-1} - t^n]$, the set of the enriched nodes will change, as new elements are being enriched and new crack segments stem. In addition, the process zone width will change according to the $\rho-$evolution laws.

2.1.1 Critical damage condition

The criterion of initiation is based on the evaluation of the damage variable d at the Gauß points of the finite element. As soon as the damage exceeds a critical damage value d_m in an element, the element is a candidate for being enriched as a master element crossed by the crack line. The initiation criterion is not sufficient to decide which of the finite elements will be newly enriched as we expect to have a set of critically damaged elements. Let I_ρ denote the set of elements where at least one of the Gauß points exceeds the first critical damage threshold d_m. In the following developments, time dependence is removed for the sake of brevity.

2.2 Direction- Tracking strategy

A threefold strategy is adopted to compute the direction of the crack: a local, a nonlocal and a local-nonlocal switch direction strategy.

Local strategy For each finite element e, we compute the principal direction of the maximum tensile principal stress of the averaged stress

$$\bar{\boldsymbol{\sigma}}_e = \frac{1}{N_g^e} \sum_{i \in \mathcal{N}_g^e} \boldsymbol{\sigma}_e(\boldsymbol{x}_{g,i}^e), \tag{20}$$

where $\mathcal{N}_g^e$ is the set of Gauß points $\boldsymbol{x}_{g,i}^e$ of element e, and N_g^e is the number of Gaußpoint in the finite element.

Nonlocal strategy A nonlocal criterion is adopted to eliminate pathological dependence of the results on mesh directionality and to smooth the crack path in those cases where the strain localization band develops as a consequence of the establishment of a stress state clearly dominated by a specific stress component. The direction of the new crack segment is computed as the principal direction of the maximum principal nonlocal stress computed as

$$\bar{\boldsymbol{\sigma}}_{NL}(\boldsymbol{x}) = \int_V \delta_\rho(\boldsymbol{x}, \boldsymbol{y}) \boldsymbol{\sigma}(\boldsymbol{y}) dV(\boldsymbol{y}). \tag{21}$$

In Eq. (21), the crack-density function δ_ρ plays the role of weighting function. In this particular case, $\ell_{\rho,M}$ is the support of δ_ρ, namely the width of the set of elements surrounding point $\boldsymbol{x}$ that are included in the computation of $\bar{\boldsymbol{\sigma}}_{NL}(\boldsymbol{x})$. Remarkably, the nonlocal stress (21) is computable in any element whether it is enriched or not, and this is useful when the element under consideration has not been enriched in the previous time set.

Local-nonlocal-switch strategy First, we compute the direction with the local and the nonlocal direction tracking criterion. Then, we require that the direction of the new crack segment ensures the least deviation with respect to the path of the existing crack line. Hence, the algorithm switches from the local to the nonlocal direction tracking criterion at each load step, so to minimize the direction variation w.r.t the crack path consolidated from the previous load step. This approach is particularly useful when we expect a deviation of the new crack line with respect to the previous one not to exceed a certain amount

of degrees and, furthermore, we do not want to give up to the nonlocal stress direction tracking criterion in certain stages of the cracking process.

The choice of the direction tracking criterion depends on the stress states arising in the particular test to be solved. Relevant aspects are deemed to be the presence of symmetry axes, the type of loading and which of the components of the stress state are involved in crack propagation. Moreover, the width of support $\ell_{\rho,M}$ of the crack density function δ_ρ for $\rho = \rho_M$ acts as an additional length parameter to decide whether distinct cracks can develop in the same neighborhood. Moreover, this length has been used as the diameter of the zone over which the nonlocal stress matrix associated with the nonlocal direction tracking criterion is computed.

2.3 Update

Among the candidate elements in I_ρ that have reached the critical damage condition, only one will host the new crack line increment. The decision is based on the following checks to be performed for each candidate element $e \in I_\rho$:

Check of crack proximity We check whether there are cracked elements in the circle of diameter $\ell_{\rho,M}$ around element e.

If there are cracked elements within $\ell_{\rho,M}$, the algorithm checks whether the crack tip belongs to the perimeter E^e including the edges of element e.

The crack tip belongs to E^e. Element e transitions from the continuous to the discontinuous setting and is enriched with the regularized extended finite element kinematics. A new crack segment is added by imposition of the crack line continuity, so that the new crack segment starts at the intersection point of the previous crack line with the relevant edge of e.

The crack tip does not belong to E^e. The element is not enriched; however, the value of the damage d in e is frozen at $d = d_m$.

No cracked elements within $\ell_{\rho,M}$. Element e is enriched and a new crack line nucleates there; e hosts the first crack segment of the newly formed independent crack. The transition of e from the standard continuum setting to the status of enriched element is activated.

End of the check of crack proximity A new element $e' \in I_\rho$ is scrutinized to verify whether it can nucleate a new crack or just orbit within the influence area of an existing one.

3 Plate with a hole

In the test [5], a plate made of a material with elastic modulus $E = 5983$ MPa and Poisson coefficient $\nu = 0.22$ is taken. Crack development is triggered by a pre-defined notch while the crack path is deviated by a hole. The geometry of the plate is shown in Fig. 2a. The damage law is characterized by $H = 0.25$ MPa and $\kappa_0 = 0.5$ MPa. The minimum and maximum values of the regularization length and damage are $\rho_m = 0.07$ mm, $d_m = 0.7$, and $\rho_M = 0.8$ mm, and $d_M = 0.95$, respectively. The contour plot of the damage d_ρ at the final cracking stage, represented by point D in Fig. 3, is shown in Fig. 2b. The contour plot has been obtained by adopting a refined mesh of triangles. The experimentally detected and the

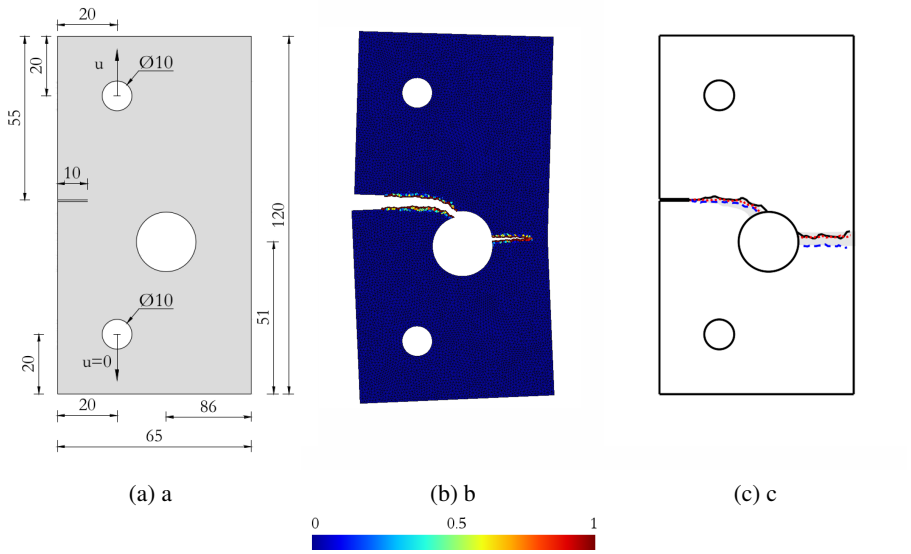

(a) a (b) b (c) c

Figure 2: a) Geometry. b) Contour plots of the evolution of the damage in the enriched zone using triangular elements with $h = 1$ mm at the load levels D indicated in Fig. 3; c) crack paths obtained with the adopted three-noded finite elements with mesh size h= 3 mm (black continuous line), h = 2 mm (blue dashed line) and h = 1 mm (red dotted line); in gray the experimentally detected cracked zone.

computed crack paths are compared in Fig. 2c for variable mesh size. In particular, we have adopted three-noded finite elements with mesh sizes h= 3 mm (black continuous line), h = 2 mm (blue dashed line) and h = 1 mm (red dotted line). The experimentally detected crack pattern is displayed in gray. We infer that the computed crack path closely follows the experimentally detected one. Furthermore, it can be remarked that we get consistent results with quite coarse meshes - $h = 1$ mm corresponds to $1/10$ of the notch length - if compared with the extremely refined meshes used in phase field models. Finally, the load-displacement results obtained with the aforementioned meshes are shown in Fig.3. It can be drawn that the obtained results are objective with respect to the mesh size.

4 CONCLUSIONS

We have presented the main lines of a newly developed strategy to track general crack paths in the framework of the regularized extended finite element method. The proposed strategy makes it possible to obtain experimentally consistent load-displacement profiles and crack paths. Our formulation naturally introduces a regularization length evolving with the damage level and a crack density function, hence suggesting certain similarities with nonlocal and phase-field models, except that damage broadening and mesh adaptivity are not an issue for the present formulation. The proposed framework is a viable alternative to available continuous-discontinuous procedures.

REFERENCES

[1] Benvenuti, E. A regularized XFEM framework for embedded cohesive interfaces. *Comput. Methods Appl. Mech. Eng.* (2008) **197**:4367–4378.

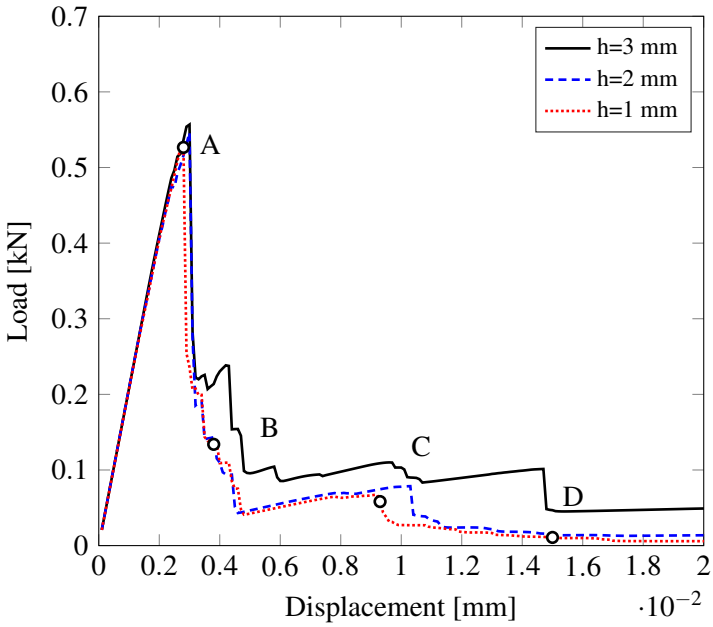

Figure 3: Plate with a hole: Load vs displacement results for variable mesh size h and using triangular elements.

[2] Jirásek, M. and Zimmermann, T. Embedded crack model. Part II: combination with smeared cracks. *Int. J. Numer. Methods Eng.* (2001) **50.6**:1291–1305.

[3] Benvenuti, E and Loret, B. and Tralli, A. A unified multifield formulation in nonlocal damage. *Eur. J. Mech. A Solids* (2004) **23**:539–559.

[4] Bourdin, B. and Francfort, G.A. and Marigo, J. A review on phase-field models of brittle fracture and a new fast hybrid formulation. *J. Elast.* (2008) **91**:5–148.

[5] Ambati, M. and Gerasimov, T. and De Lorenzis, L. A review on phase-field models of brittle fracture and a new fast hybrid formulation.*Comput. Mech.* (2015) **55**: 383–405.

[6] Turon, A. and Dávila, C.G. and Camanho, P.P. and Costa, J. An engineering solution for mesh size effects in the simulation of delamination using cohesive zone models. *Eng. Fract. Mech.* (2007) **74**:1665–1682.

[7] Belytschko, T and Gracie, R. and Ventura, G. A review of extended/generalized finite element methods for material modeling. *Model. Simul. Mat. Sci. Eng.* (2009) **17.4**:043001.

[8] Sukumar, N. and Dolbow, J.E. and Moës, N. Extended finite element method in computational fracture mechanics: a retrospective examination. *Int. J. Fract.* (2015) **196**:189–206.

[9] Unger, J.F. and Eckardt, S. and Könke, C. Modelling of cohesive crack growth in concrete structures with the extended finite element method. *Comput. Methods Appl. Mech. Eng.* (2007) **196.41**:4087–4100.

[10] Geelen, R.J.M. and Liu, Y. and Dolbow, J.E. and Rodríguez-Ferran, A. An optimization-based phase-field method for continuous-discontinuous crack propagation. *Int. J. Numer. Methods Eng.* (2018) **116**:1–20.

[11] Benvenuti, E and Tralli, A. Simulation of finite-width process zone in concrete-like materials by means of a regularized extended finite element model. *Comput. Mech.* (2012) **50**:479–497.

[12] Benvenuti, E and Ventura, G. and Ponara, N. and Tralli, A. Variationally consistent extended FE model for 3D planar and curved imperfect interfaces. *Comput. Methods Appl. Mech. Eng.* (2013) **267**:434–457.

[13] Benvenuti, E. XFEM with equivalent eigenstrain for matrix–inclusion interfaces. *Comput. Mech.* (2014) **53**:893–908.

[14] Benvenuti, E and Orlando, N. Intermediate flexural detachment in FRP-plated concrete beams through a 3D mechanism-based regularized eXtended Finite Element Method. *Compos. B Eng.* (2018) **145**:281–293.

[15] Benvenuti, E and Orlando, N. and Gebhardt, C. and Kaliske, M. An orthotropic multi-surface damage-plasticity fe-formulation for wood: Part II - Numerical Applications. *Comput. & Struct.* (2020) **240**:106350.

[16] Benvenuti, E and Orlando, N. A new framework for crack tracking in elastodamaging materials through the regularized extended finite element method. (2021) forthcoming.

[17] Ambrosio, L. and Tortorelli, V.M. On the approximation of free discontinuity problems. *Boll. Unione Mat. Ital.* (1992) **6B:1**:105–123.

[18] Braides, A. *A handbook of* Γ*-convergence* In *Handbook of Differential Equations. Stationary Partial Differential Equations*. Elsevier, Vol. 3, (2006).

[19] Benvenuti, E and Ventura, G. and Ponara, N. and Tralli, A. Accuracy of three-dimensional analysis of regularized singularities. *Int. J. Numer. Methods Eng.* (2015) **101**:29–53.

[20] Ventura, G. and Budyn, E. and Belytschko, T. Vector level sets for description of propagating cracks in finite elements. *Int. J. Numer. Methods Eng.* (2003) **58**:1571–1592.

[21] Benvenuti, E. Damage integration in the strain space. *Int. J. Solids. Struct.* (2004) **41**: 3167–3191.

[22] Cervera, M. and Chiumenti, M. Mesh objective tensile cracking via a local continuum damage model and a crack tracking technique. *Comput. Methods Appl. Mech. Eng.* (2006) **196**:304–320.